

Attenuation of Nano-TiO₂ Induced Genotoxicity, Mutagenicity and Apoptosis by Chlorophyllin in Mice Cardiac Cells

Hanan Ramadan Hamad Mohamed

Lecturer of Genetics, Zoology Department, Faculty of Science, Cairo University, Egypt

Abstract: *Despite uses of titanium dioxide (TiO₂) particles in various consumer and medical products therapy increasing human daily exposure, little studies were conducted on its cardiotoxicity. Thus, this study was designed to investigate the possible modulation of nano-TiO₂ induced genotoxicity, mutagenicity and apoptosis by chlorophyllin (CHL) coadministration in mice cardiac cells. Mice were injected into the abdominal cavity with TiO₂ (500, 1000 and 2000 mg/kg b.w) suspended either in deionized dist. water or in CHL (40 mg/kg b.w) solution for five consecutive days and sacrificed 24 hour after the last injections. CHL co-administration resulting in significant reductions in tail length, %DNA in tail and tail moment that was highly elevated in nano-TiO₂ treated groups in a dose dependent manner, also the appearance of both apoptotic fragmented Laddered and smeared DNA on agarose gel was returned to the normal unfragmented appearance. The observed dose dependent high incidence of mutations inductions in p53 exons (5-8) and myocardial cells infiltrations by inflammatory cells, hemorrhage and congested blood vessels by nano-titanium was attenuated by CHL co-administration. Finally, CHL improved the antioxidant defense system indicated by significant reduction in malondialdehyde level and increases in reduced glutathione level and glutathione peroxidase activity that were disrupted in nano-titanium treated groups. In conclusion: nano-TiO₂ particles induced genotoxicity, mutagenicity and apoptosis were attenuated by CHL co-administration in mice cardiac cells. It is recommended for further studies to detect the CHL dose that completely normalize nano-titanium induced cardiotoxicity.*

Keywords: TiO₂ nanoparticles, genotoxicity, mutagenicity, p53, apoptosis, mice cardiac cell

1. Introduction

Human daily exposure to titanium dioxide nanoparticles (TiO₂) are potentially increased due to their widely used in many consumer products: toothpastes, sunscreens, cosmetics, food products, pharmaceuticals, and nanomedical reagents. Currently, TiO₂ nanoparticles are being used as bactericidal agents in artificial heart valves and have a potential medical application in cardiovascular imaging and disease treatment due to their high photocatalytic activity [1,2].

Accumulation of metal nanoparticles has been observed in all organs in vivo: TiO₂ could be absorbed through various routes penetration into the body, and distributed in the important organs such as lung, lymph nodes, brain, heart, liver and kidney [3-7]. Moreover, Chen and his coworkers [7] showed that nano-TiO₂ particles could transport to and deposit in other tissues: spleen, heart, lung liver and kidney after intraperitoneal injection as assessed by distribution experiment. Consequently, the adverse effects of TiO₂ are intensively investigated with increasing interest in its potential toxicity.

Therefore, recent studies concerned on the toxicological effects of nano-titanium both in vitro and in vivo. Despite excessive studies on nano-TiO₂ induced toxicity has been done; few studies were concerned on nano-titanium cardiotoxicity. In *in vitro* nano-titanium has been shown to damage cardiac cells [1] and primary cardiac myocytes of rat [8]. Recent in vivo studies have confirmed that TiO₂ nanoparticles accumulated in the heart triggers DNA damage and oxidative stress in mice and rat cardiac cells [9-12] that evidenced the close association between nano-titanium toxicity and cardiovascular adverse effects such as myocardial infarction.

Several studies indicated that nano-titanium particles injected intraperitoneally caused serious damage to myocardium function as indicated by significant increases in the activities of aspartate aminotransferase, creatine kinase, lactate dehydrogenase, and alpha-hydroxybutyrate dehydrogenase, indicator of the myocardium function [9,13]. In addition, reactive oxygen species-mediated (ROS) toxicity by TiO₂ have been reported by numerous studies as ROS play an important role in the pathogenesis of atherosclerosis and several other cardiovascular diseases [4,11,14]. Moreover, the study of Sheng *et al.*, [14] showed that TiO₂ exposure increased malondialdehyde, carbonyl and 8-oxyhydroxy deoxyguanine (8-OHdG) levels as degradation products of lipid, protein, and DNA peroxidation, respectively, and reactive oxygen species (superoxide radicals, hydrogen peroxide) production and attenuated the activities of antioxidative enzymes: superoxide dismutase, ascorbate peroxidase, glutathione reductase, glutathione-S-transferase, and levels of antioxidants including ascorbic acid, glutathione, and thiol in heart resulting in impairment of cardiovascular system in mice.

As characteristics of TiO₂ can be modified by several methods to improve their performance and naturally occurring compounds have protective effects against environmental mutagens/carcinogens and endogenous mutagens [15,16], natural compounds were used in this study as one possible way to reduce TiO₂ induced cardiotoxicity. Chlorophyllin (CHL) is a sodium-copper salt derivative of chlorophyll where the central nucleus of magnesium is substituted by another metal such as copper, iron or cobalt and where the phytyl and methyl ester groups are substituted by sodium or potassium [17] converting it into water soluble. Its antigenotoxic, anticlastogenic, antimutagenic and anticarcinogenic

potential has been shown both in vitro and in vivo ([18-21]. In the study of García-Rodríguez *et al.* [22] CHL administered prior to chromium trioxide (CrO₃) treatment resulted in a significant decrease in the frequency of micronuclei observed 12 hours after CrO₃ treatment in rat while CHL itself did not induce any change in the micronuclei frequency.

Moreover, over the past decade, researchers have demonstrated the increased importance of CHL as a potent antioxidant and it has been shown to be effective in scavenging of ROS [20,23]. Ibrahim *et al.* [24] evidenced the antioxidative property of CHL by the effective prevention of oxidative damage caused by cyclophosphamide and benzo[a]pyrene in male albino rats. Therefore, the present study was designed to nano-TiO₂ induced genotoxicity, mutagenicity and apoptosis by CHL co-administration in mice cardiac cells. Comet, ladder DNA fragmentation and SSCP assays and histological examination were used as genotoxicity and histopathological end points respectively. Moreover, estimation of some biochemical parameters of oxidative stress was done to shed more light on oxidative stress inductions.

2. Materials and Methods

2.1 Animals

Male Swiss Webster mice weighting 20-25 gm and aged 10-12 weeks were obtained from the animal house of National Organization for Drug Control and Research (NODCAR). Animals were supplied with standard diet pellets and water that were given ad *Libitum*, kept in plastic cages for 7 days to be accommodated with our laboratory conditions before being treated.

2.2 Chemicals

All chemicals were purchased from Sigma chemical Co., St. Louis, MO, USA Company. TiO₂ were purchased in the form of white powder with purity 99.5%, CAS number 13463-67-7. This purchased nano-titanium was in the form of rutile and anatase mixture with particle size of <100 nm using Brunauer-Emmett-Teller (BET) method and <50 nm using X-ray diffraction method. It was suspended in either deionized distilled water or CHL solution to prepare the tested doses (500, 1000 and 2000 mg/kg b.w) (Guo *et al.*, 2009; Faddah *et al.*, 2013). CHL was purchased as green powder and dissolved into deionized dist. water to prepare the desired dose (40 mg/kg bw) for injection according to (Gradecka-Meesters *et al.*, 2011).

2.3 Preparation and Characterization of Nano TiO₂ for Injection

TiO₂ nanoparticles were ultra-sonicated in either deionized water or CHL solution using the biologics ultrasonic homogenizer (Model 150VT) immediately before the processes of characterization and administration. Characterization of nano- TiO₂ particles in both dry and liquified states was done using X-ray diffraction (XRD) and transmission electron microscopy (TEM),

respectively. First: at room temperature XRD patterns of TiO₂ were obtained using charge-coupled device (CCD) diffractometer (XPRT- PRO-PANalytical-Netherland) and Ni-filtered Cu K α radiation ($k = 1.54056 \text{ \AA}$) in the range of 20 - 70° at 45 keV. Thus, the crystal phase could be identified and average crystallite size could be calculated by The Scherrer's relationship ($D = 0.9k/B\cos\theta$) where, k is the wavelength of X-ray, B is the broadening of diffraction line measured as half of its maximum intensity in radians and θ is the Bragg's diffraction angle.

Moreover, TEM was used to determine the particle size and morphology of the powder in suspension state. Nano-TiO₂ particles were suspended in either Milli-Q water or CHL solution and sonicated at 40 W for 20 minutes and dropped TiO₂ suspensions on carbon-coated copper TEM grids then dried prior to measurement. TEM (a Tecnai G20, Super twin, double tilt) operated at an accelerating voltage at 200 kV. Results are expressed as mean \pm SE.

2.4 Treatment schedule

All experiments were conducted in accordance with the guidelines approved by the local animal care and use committee at Cairo University. Animals were divided randomly into 8 groups, five animals for each. All animals were injected intraperitoneally (i.p.) for five consecutive days. Negative control group (group 1) and CHL control group (group 2) were injected with dist. H₂O and CHL (40 mg/kg/day) respectively. The other 6 groups were injected with TiO₂ nanoparticles different doses (500, 1000 and 2000 mg/kg b.w/day) suspended in either deionized water (groups 3, 4 and 5) or in CHL solution (groups 6, 7 and 8). All animals were sacrificed 24 hour after the last injection by cervical dislocation as a physical Euthanasia method of laboratory animals death because anaesthetic agents affect cardiovascular, respiratory and thermo-regulatory mechanism in addition to central nervous system thus it can't be applied in this study.

2.5 Genotoxicity assays

2.5.1 Alkaline comet assay

This assay was conducted to detect single and double strand breaks inductions by nano-TiO₂ particles in myocardial cells. It was performed according to Tice *et al.* [25] with minor modifications. The extent of DNA migration for each sample was determined by simultaneous image capture and scoring of 100 cells at 400 x magnification using Comet 5 image analysis software developed by Kinetic Imaging, Ltd. (Liverpool, UK). The extent of DNA damage was evaluated according to the following endpoints measurements: Tail length: it is used to evaluate the extent of DNA damage away from the nucleus and expressed in μm , % DNA in tail: intensity of all tail pixels divided by the total intensity of all pixels in the Comet and tail moment = tail length \times %DNA in tail/100.

2.5.2 DNA fragmentation assay

According to Sriram *et al* [26] about 1×10^6 cells were lysed in 250 μL cell lysis buffer containing 50 mM Tris

HCl, pH 8.0, 10 mM ethylenediaminetetraacetic acid, 0.1 M NaCl, and 0.5% sodium dodecyl sulfate. Then incubated with 0.5 mg/mL RNase A at 37°C for one hour, and finally with 0.2 mg/mL proteinase K at 50°C overnight. Phenol extraction of this mixture was carried out, and DNA in the aqueous phase was precipitated by 25 µL (1/10 volume) of 7.5 M ammonium acetate and 250 µL (1/1 volume) isopropanol. Fragmentized DNA was electrophoresed in a 1% agarose gel containing 1 µg/mL ethidium bromide at 70 V, and visualized by UV transilluminator, followed by photography.

2.5.3 Single Strand Conformation Polymorphism (SSCP) Analysis

2.5.3.1 Isolation of Genomic DNA

DNA pellet was extracted according to the method described by Biase *et al.*, [27], with slight modifications. After tissue homogenization (200 mg) in sterile salt cold homogenizing buffer (50 mM Tris-HCl, pH 8.0; 25mM EDTA 0.4 M NaCl), 20% SDS and proteinase K (20 mg/ml) were added, mixed well and incubated at 55°C in heating block overnight with shaking for complete denaturation and solubilization of protein. After incubation, proteins and cellular debris were precipitated by adding 6 M NaCl (NaCl saturated samples were vortexed for 30 seconds for mixing). Samples were kept at 4°C for 20 min, followed by centrifugation at 14,000 rpm for 15 minutes at room temperature. The supernatant was transferred to fresh tube, an equal volume of cold 100% ethanol was added for complete precipitation of DNA, left overnight at 4°C and finally centrifuged at 14,000 rpm for 20 minute at 4°C. DNA pellet was washed in 200-700 µl of 100% cold ethanol. Pour off the ethanol and briefly spin the sample to keep the pellet at the bottom of the tube. The DNA pellet was washed twice with 70% ethanol as above, dried and finally resuspended pellets in 100-200 µl of sterile deionized distilled water.

2.5.3.2 Polymerase Chain Reaction (PCR) Amplification

For SSCP analysis of *p53* exons 5– 8, PCR of genomic DNA was performed. Four pairs of PCR primers for mouse *p53* exons 5-8 (Table 1) were selected based on the published sequence [28]. 250 ng of extracted DNA, 50 pmole of both forward and reverse primers and 2 x master mixes were mixed. Samples were initially denaturated at 95 C for 5 mins. Then, Thirty nine cycles of denaturation (95°C), annealing (58 °C for exons 5 and 8), (62°C for exons 6 and 7), and extension (72°C) were done. Final extension at 72° C for 10 mins was necessary, for complete amplification. PCR products were separated and visualized by electrophoresis through 2% ethidium bromide-treated agarose gel using UV transilluminator (Stratagene, USA).

2.5.3.3 SSCP analysis for PCR products

SSCP is a widely used method for mutation detection because of its simplicity and versatility. a 5 µl aliquot of purified PCR product mixed with 5 µl of denaturing-loading dye (95% formamide, 0.1% bromophenol blue,

0.1% Xylene cyanol FF and 0.5 µl 15% Ficoll) and 5 µl of TE buffer was heat denaturated at 94°C for 7 min. and then chilled on ice for 10 mins [29]. Samples were electrophoresed at 90 volt till the dye reached the bottom of the gel (about 45 mins) and stained for 10 mins in 100 ml of 1x TBE with ethidium bromide to visualize the DNA bands with the aid of shaking. Finally, gel was examined using UV transilluminator and photograph by Polaroid camera (PolaroidMP4 Land Camera).

Table 1: Oligonucleotide primers used for the *p53* gene amplification

Exon	Length	Stand	Sequence
5	184	Sense	TACTCTCCTCCCCTCAATAAG
		Antisense	ACCATCGGAGCAGCCCTCAT
6	113	Sense	CTGGCTCCTCCCAGCATCTT
		Antisense	CTCGGGTGGCTCATAAGGTAC
7	110	Sense	GCCGGCTCTGAGTATACCACC
		Antisense	CTGGAGTCTTCCAGTGTGATG
8	137	Sense	GCGAACCTTCTGGGACGGGAC
		Antisense	TCTCTTTGCGTCCCCTGGGGG

2.6 Histopathological Examination

For pathological studies fresh portions of heart were cut rapidly, fixed in neutral buffered formalin (10%), dehydrated using grades of ethanol (70%, 80%, 90%, 95%, and 100%) and followed by clearing the samples in two changes of xylene. Then impregnated with two changes of molten paraffin wax, embedded, and blocked out. Finally sliced the tissue sections (4–5 µm thickness), and placed on glass slides. After hematoxylin–eosin staining, the stained sections were evaluated by a histopathologist unaware of the treatments using light microscopy (U-III Multi-point Sensor System; Nikon, Tokyo, Japan).

2.7 Oxidative stress assays

2.7.1 Malondialdehyde (MDA) level

Cardiac MDA level was measured using method described by Ohkawa *et al.* [30] depending on thiobarbituric acid (TBA) reaction with malondialdehyde (MDA) in acidic medium at temperature of 95°C for 30 min. to form thiobarbituric acid reactive product. The absorbance of the resultant pink product was measured spectrophotometrically at 534 nm. Results were expressed as nmol/g tissue used.

2.5.2 Reduced glutathione (GSH) level

Ellman, [31] method was used to estimate cardiac GSH level based on the reduction of Ellman's reagent [5, 5' dithio bis-(2-nitrobenzoic acid)] with glutathione (GSH) to form 1 mol of 2-nitro-5-mercaptobenzoic acid (yellow compound) per mol of GSH. The reduced chromogen is directly proportional to GSH concentration and its absorbance was determined at 412 nm. Results were expressed as µmol/g tissue used.

2.7.3 Glutathione peroxidase (GPx) activity

According to Paglia and Valentine [32] GPx activity was measured depending on the reaction in which oxidized glutathione (GSSG), produced upon reduction of peroxides, and recycled to its reduced state by the enzyme glutathione reductase. The oxidation of NADPH to NADP^+ is accompanied by a decrease in absorbance at 340 nm (A_{340}) providing a spectrophotometric means for monitoring GPx enzyme activity. The rate of decrease in the A_{340} is directly proportional to the GPx activity in the sample. Results were expressed as μg tissue.

2.8 Statistical analysis

Results were expressed as mean \pm standard error (S.E.) Statistical analysis was performed using the T-test to test the significance level between groups. All statistics were carried out using Statistical Analysis Systems (SAS) program [33] ®. Moreover, regression analysis was carried out to test the correlation between different nano-titanium doses and its toxicity.

3. Results

3.1 TiO_2 nanoparticles characterization

As shown in the X-ray diffraction pattern (Fig.1A) TiO_2 nanoparticles are a mixture of rutile and anatase by the peaks that were corresponding with the tetragonal rutile and anatase structure of nano- TiO_2 particles. No impurity phase was observed in the sample. The calculated average crystallite size using Debye Scherrer's formula was about 46 nm in agreement with the recorded nano-titanium particle size using TEM. Despite small agglomerates were observed in aqueous solution using TEM, the TiO_2 nanoparticles were still in the nanoscale range with the average size of about 47.33 ± 6.07 nm in H_2O and 41.44 ± 5.73 nm in CHL (Fig. 1B). As shown in Fig. 1C particles size in CHL solution was slightly smaller than that in H_2O but still statistically unchanged. Moreover, TiO_2 nanoparticles are crystallites with polyhedral morphologies thus increasing its surface area and its activity.

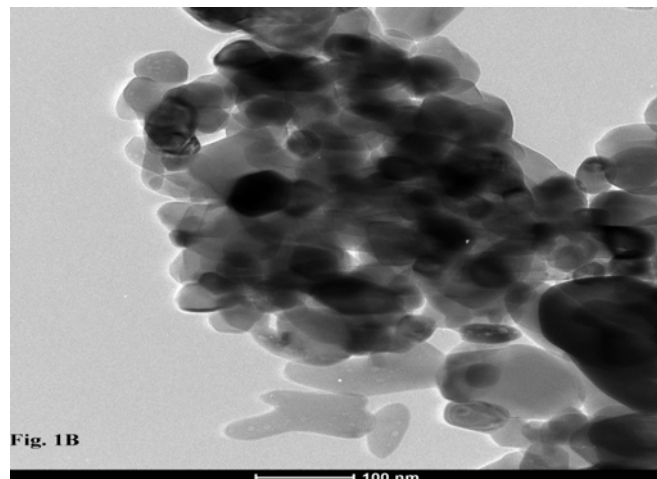
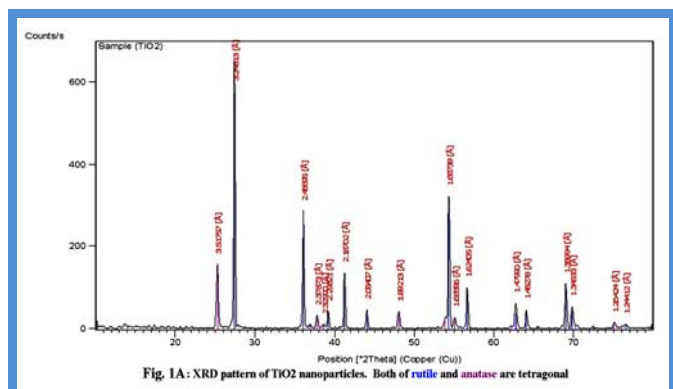


Figure 1B: Transmission electron microscopy (TEM) image

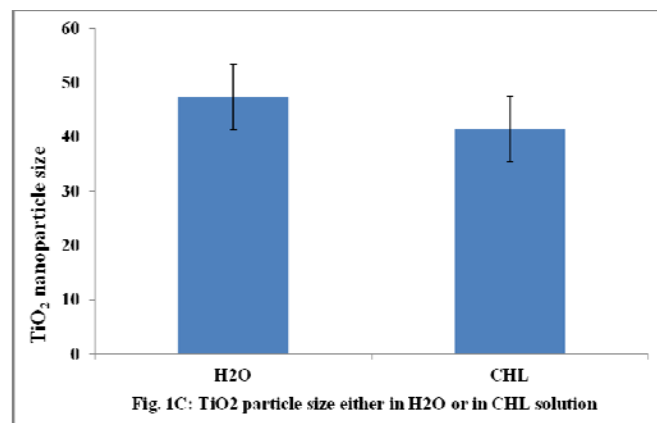


Figure 1: Characterization of TiO_2 nanoparticles

3.2 Comet assay

Various grades of DNA damage were observed and shown in Fig. 2A. As shown in table 2 no any statistical significant in tail length, %DNA in tail and tail moment was observed in group treated with CHL but DNA damage induction by nano-titanium different doses was indicated by the statistical significant increases in tail length, %DNA in tail and tail moment ($p < 0.001$) compared with the negative control. However, CHL co-administration resulted in statistical significant decreases ($p < 0.001$) in nano- TiO_2 induced DNA damage (groups 6-8) compared with titanium treated groups (3-5) at the three tested doses and reached to the negative control level. Strong positive correlations between DNA damage inductions and different TiO_2 was evidenced by the regression analysis curves (Fig. 2B).

Table 2: DNA damage inductions and TiO₂ nanoparticles different doses injected alone or with CHL in mice cardiac cells

Group	Treatment (Dose mg/kg)	Tail length (µm)	%DNA in tail	Tail moment
1	Negative control	2.45 ± 0.13	29.08 ± 0.89	0.80 ± 0.03
2	CHL	2.35 ± 0.11	25.24 ± 1.85	0.69 ± 0.07
3	TiO ₂ (500)	4.41 ± 0.26 ^{a***}	42.92 ± 0.71 ^{a***}	2.28 ± 0.09 ^{a***}
4	TiO ₂ (1000)	5.78 ± 0.43 ^{a***}	42.55 ± 0.96 ^{a***}	2.83 ± 0.28 ^{a***}
5	TiO ₂ (2000)	7.09 ± 0.20 ^{a***}	50.3 ± 1.06 ^{a***}	3.83 ± 0.10 ^{a***}
6	TiO ₂ (500) + CHL (40)	2.46 ± 0.10 ^{b***}	26.81 ± 2.30 ^{b***}	0.74 ± 0.06 ^{b***}
7	TiO ₂ (1000) + CHL (40)	2.94 ± 0.24 ^{b***}	28.91 ± 1.73 ^{b***}	0.95 ± 0.07 ^{b***}
8	TiO ₂ (2000) + CHL (40)	2.72 ± 0.15 ^{b***}	29.60 ± 0.75 ^{b***}	0.90 ± 0.05 ^{b***}

Results are expressed as mean ± SE. a & b: statistically compared with negative control group and comparable TiO₂ alone treated group, respectively, at p<0.001.

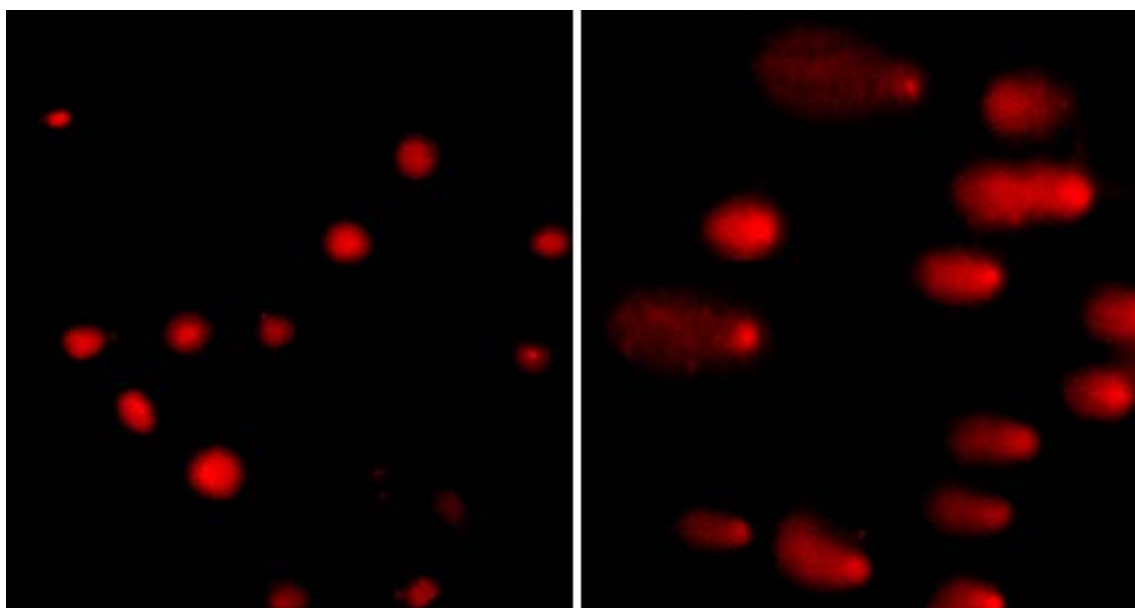
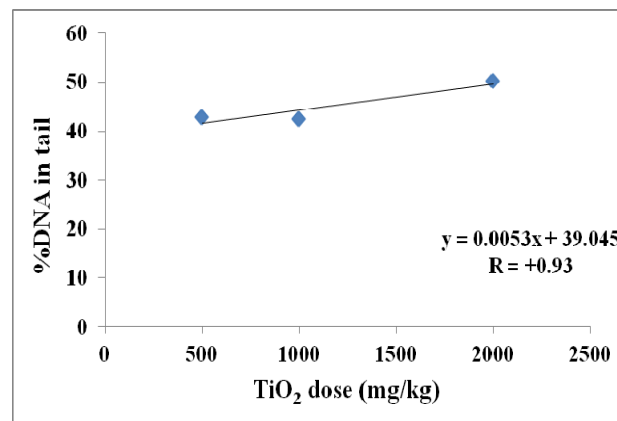
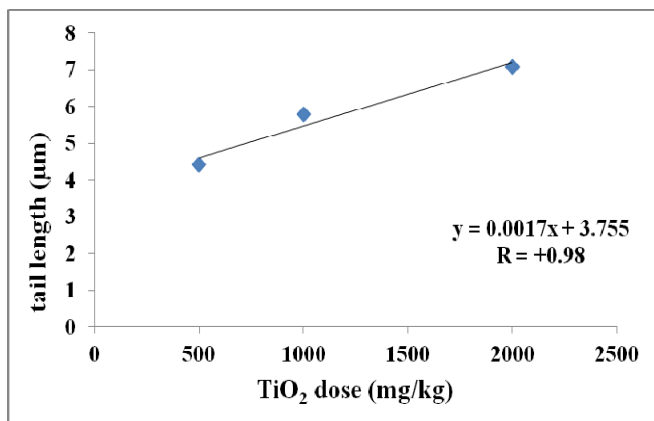


Figure 2A: Representative micrograph for undamaged (Left side) and damaged (Right side) DNA in different groups



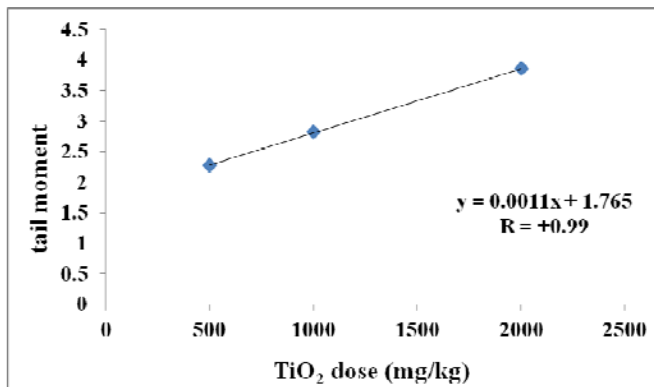


Figure 2B: Regression lines and correlation coefficients for tail length, %DNA tail and tail moment of mice injected by TiO₂ different doses. Results are expressed as mean

3.3 DNA fragmentation

Pulsed field gel electrophoresis was used for qualitative analysis of DNA fragmentation and summarized in Fig. 3. CHL did not induce any DNA fragmentation as CHL treated group has banding pattern similar to that of the negative control group with neither a DNA ladder nor a smear on the gel. On contrary, DNA fragmentation by the nano-TiO₂ particles was evidenced by the appearance of fragmented DNA in the form of both ladder and smeared DNA fragments at the three tested doses (Lanes 3-5) in a dose-dependent manner as only smeared DNA was detected at the lowest dose (500 mg/kg) while both of ladder and smeared DNA were observed at the higher titanium doses (1000 and 2000 mg/kg). This DNA damage was markedly reduced by CHL co-administration as indicated by disappearance of both ladder and smeared DNA fragments completely at TiO₂ (500 mg/kg) but still slightly exists at both the higher doses (TiO₂ 1000 and 2000 mg/g) (Lanes 6-8).

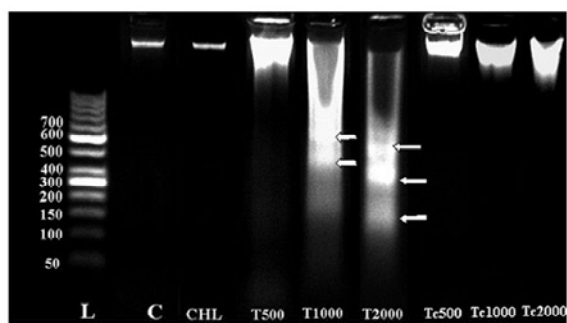


Fig. 3: DNA fragmentation assay showing apoptotic DNA fragmentation of mice treated with TiO₂ different doses alone (T) and with CHL (Tc) compared with DNA ladder (L) marker and negative control group (C). Arrows indicated the appearance of fragmented DNA.

3.4 SSCP analysis

Fig. 4A showed that the electrophoresed PCR products of the four p53 exons (5-8) have a size of 184, 113, 110 and 137 bp, respectively, which confirming the successful amplification of the interested bands. Representative cases for SSCP analysis are shown in Fig. 4B. As shown in table 3 three mice were examined per each dose and four exons per each animal, so total examination is equal to twelve.

SSCP analysis of exons 5–8 revealed altered banding patterns that confirming the inductions of mutations in groups treated with nano-TiO₂ particles in a dose dependent manner. Three (one in each of exons 6, 7 and 8), six (two in each of exons 7&8 and one in each of exons 5&6) and nine (two in each of exons 5, 6 and 8 and three in exon 7) mutations out of twelve (25%), (50%) and (75%) were observed for TiO₂ (500, 1000 and 2000 mg/kg), respectively (Table 3). However, mutation frequencies were highly decreased after CHL coadministration with TiO₂ nanoparticles and reached the negative control level except in exons 8 and 6 were still mutated (17%) two out of twelve at the highest TiO₂ dose (2000 mg/kg).

Table 3: Incidence of mutations inductions in p53 exons (5-8) in cardiac Cells of mice injected i.p. with TiO₂ nanoparticles suspended in H₂O or in CHL

Exon	No. of examined mice	No of mutations observed at different TiO ₂ doses					
		TiO ₂ alone			TiO ₂ + CHL		
		500 mg	1000 mg	2000 mg	500 mg	1000 mg	2000 mg
Exon 5	3	1	2	2	0	0	1
Exon 6	3	0	1	2	0	0	0
Exon 7	3	1	1	2	0	0	1
Exon 8	3	1	2	3	0	0	0
total	12	3	6	9	0	0	2

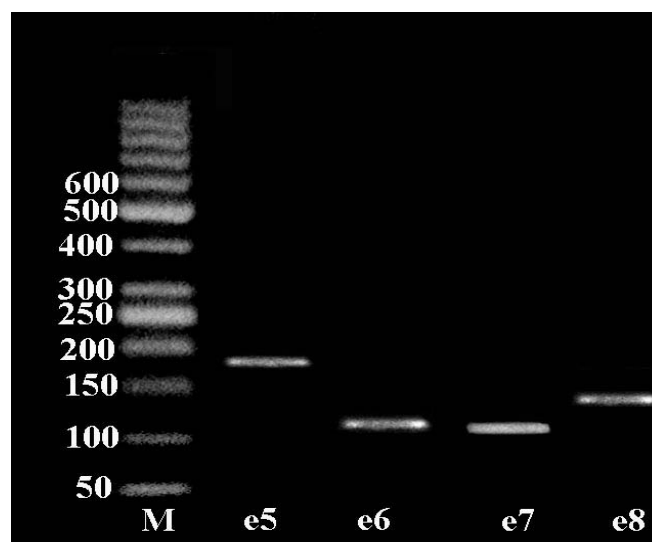
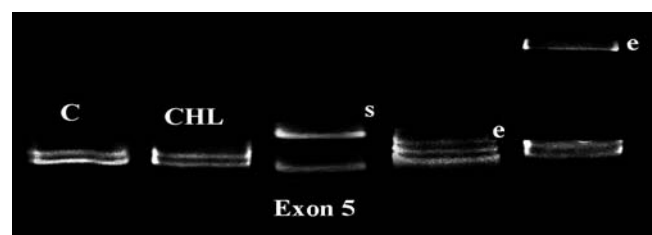


Figure 4A: Representative photo for PCR products of p53 exons (e5-e8)



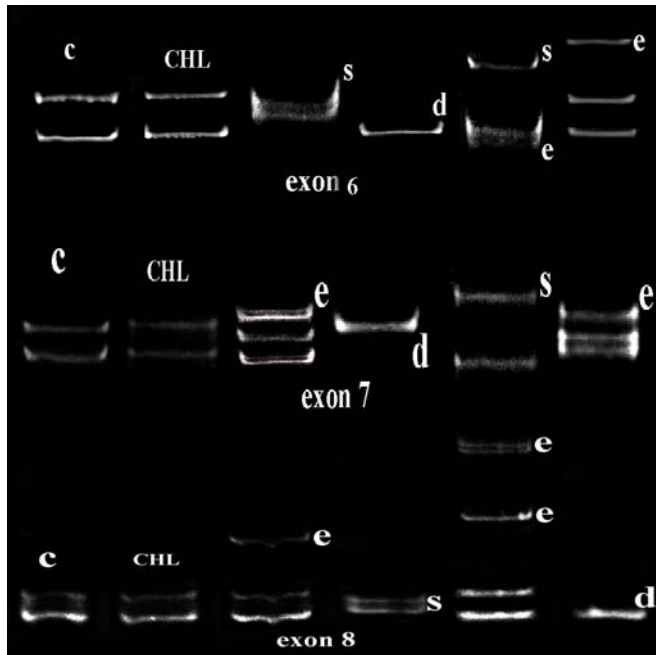


Figure 4B: Representative photomicrograph for the detected mutations: extra band (e), shift (s) and deletion (d) in four p53 exons (5-8) of the treated mice (T) compared with negative control group (c)

3.5 Histopathological Analysis

Histopathological examinations of CHL treated animals showing apparently healthy myocardial muscles without any abnormality in the heart architecture compared with the negative control group (Fig. 5). In contrast, the heart of nano-TiO₂ treated groups had abnormal pathology changes compared with the control increasing gradually with increasing titanium dose as shown by the appearance of diffuse muscle hyalinosis and congested blood vessel in the low TiO₂ group (500 mg/kg), diffuse muscle hyalinosis, diffuse muscular edema, hemorrhage and focal leucocytic infiltration in the medium TiO₂ group (1000 mg/kg) and zenker's necrosis of muscles with mononuclear cells infiltration in the high TiO₂ group (2000 mg/kg). On contrary, CHL co-administration with TiO₂ nanoparticles returned myocardial muscles to their healthy apparent at the TiO₂ dose (500 mg/kg) and with slightly congested blood vessel at TiO₂ (1000 mg/kg) but regression of the infiltrated mononuclear cells were observed at TiO₂ (2000 mg/kg).

3.6 Oxidative Stress Assays

Results are summarized in Table 4. CHL did not induce any statistical significant change in the MDA and GSH levels and Gpx activity compared with the negative control values. Despite, the disturbance in the antioxidant defense system by nano-TiO₂ was indicated by the observed statistical significant elevations ($P < 0.001$) in MDA level TiO₂ by about 148%, 349 and 522% and decreases in both of GSH level by 30%, 44% and 64% and Gpx activity by 64%, 75% and 86% at the different titanium dose 500, 1000 and 2000 mg/kg), respectively, compared with the negative control values. Strong coefficient correlation between nano-TiO₂ and MDA and oxidative stress biomarkers was indicated by regression analysis curves (Fig. 6) and evidenced dose dependent manner of nano-titanium. CHL co-administration ameliorated the antioxidant defense system by the statistically significantly reduction in the MDA level ($P < 0.001$) by about 61%, 76% and 81%, and increases in both of GSH level by 42%, 59% and 140% and GPx activity by 188%, 272% and 500% compared with the comparable TiO₂ treated groups and even though reached to the negative control level with no statistical significant differences.

Table 4: MDA and GSH levels and Gpx activity in myocardial muscles of mice injected i.p. with TiO₂ suspended either in H₂O or in CHL solution.

Group	Treatment (Dose mg/kg)	MDA level (nmol/g tissue)	GSH level (μmol/g tissue)	Gpx activity (U/g tissue)
1	Negative control	35.6 ± 1.17	1.71 ± 0.26	2.73 ± 0.36
2	CHL	36.4 ± 1.47	1.69 ± 0.05	2.75 ± 0.34
3	TiO ₂ (500)	88.2 ± 7.68 ^{****}	1.20 ± 0.14	0.97 ± 0.17 ^{***}
4	TiO ₂ (1000)	159.80 ± 18.25 ^{****}	0.96 ± 0.03 ^{***}	0.68 ± 0.13 ^{***}
5	TiO ₂ (2000)	221.40 ± 15.74 ^{****}	0.62 ± 0.04 ^{***}	0.39 ± 0.06 ^{****}
6	TiO ₂ (500) + CHL (40)	34.20 ± 1.65 ^{****}	1.70 ± 0.04 ^{b**}	2.79 ± 0.45 ^{b**}
7	TiO ₂ (1000) + CHL (40)	38.4 ± 4.87 ^{b***}	1.53 ± 0.07 ^{b***}	2.53 ± 0.16 ^{b***}
8	TiO ₂ (2000) + CHL (40)	42.6 ± 3.44 ^{b***}	1.49 ± 0.06 ^{b***}	2.34 ± 0.19 ^{b***}

Results are expressed as mean ± SE. a & b: statistically compared with negative control and comparable TiO₂ treated groups, respectively, at $p < 0.05$ (*), $p < 0.01$ (**) and $p < 0.001$ (***).

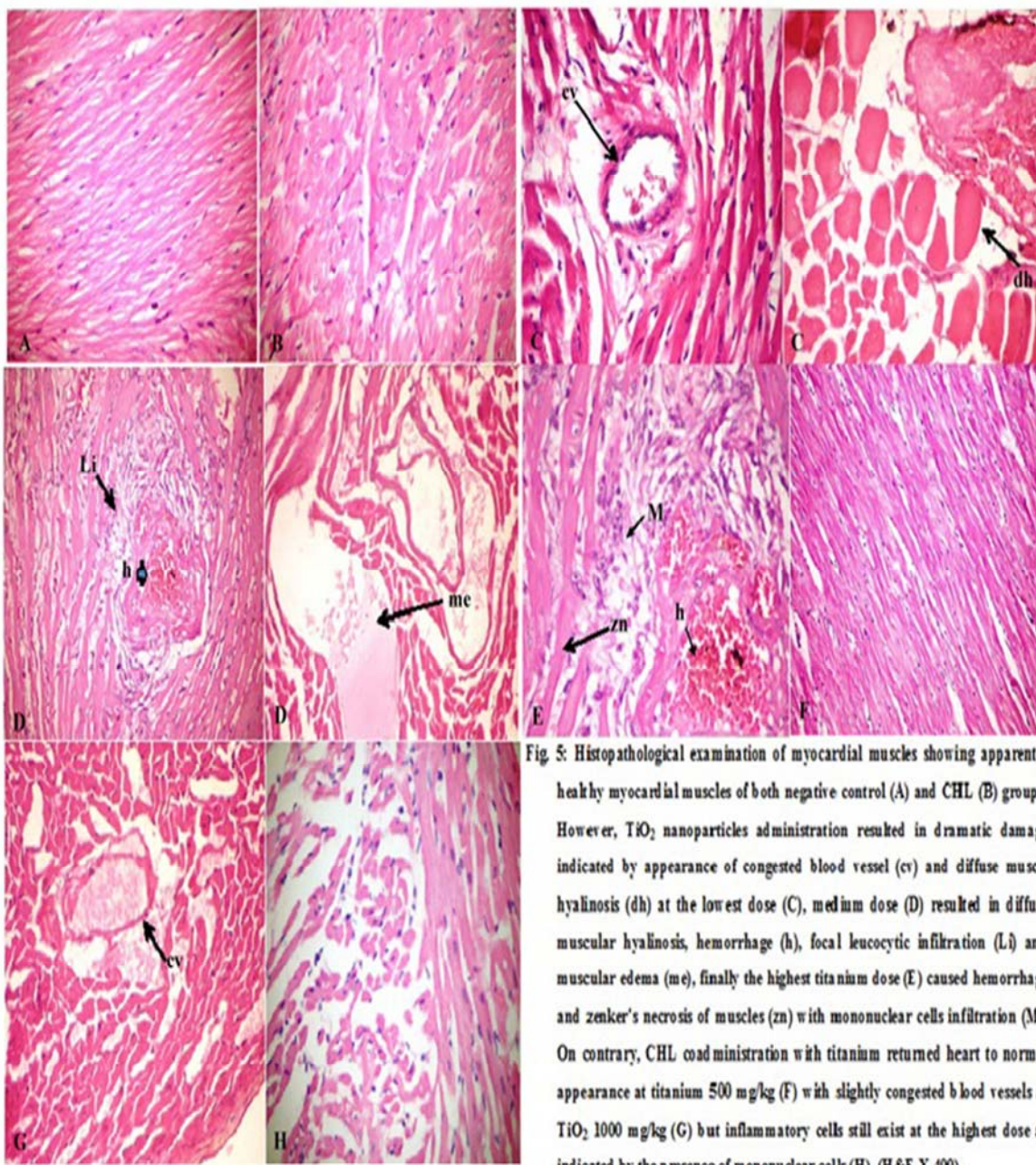
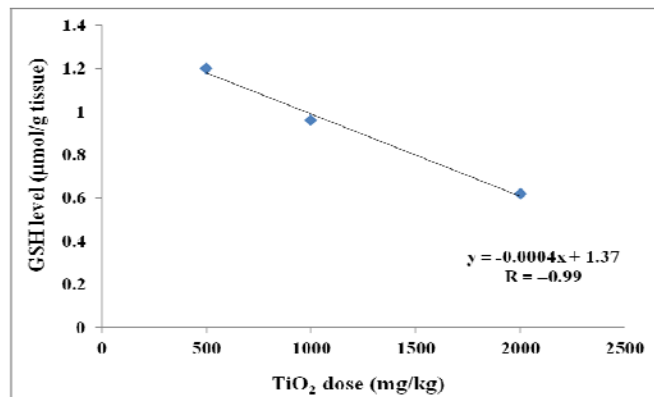
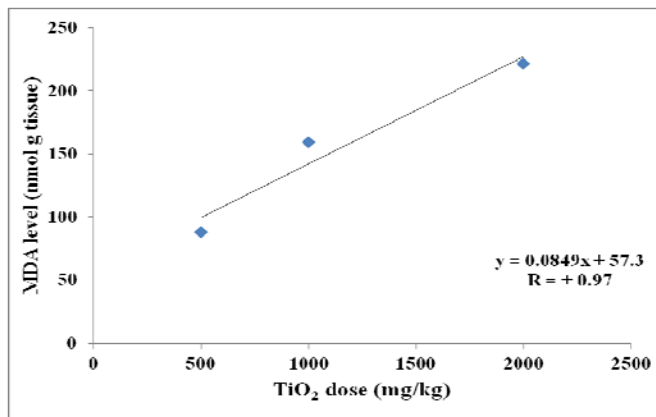


Fig. 5: Histopathological examination of myocardial muscles showing apparently healthy myocardial muscles of both negative control (A) and CHL (B) groups. However, TiO₂ nanoparticles administration resulted in dramatic damage indicated by appearance of congested blood vessel (cv) and diffuse muscle hyalinosis (dh) at the lowest dose (C), medium dose (D) resulted in diffuse muscular hyalinosis, hemorrhage (h) and focal leucocytic infiltration (Li) and muscular edema (me), finally the highest titanium dose (E) caused hemorrhage and zenker's necrosis of muscles (zn) with mononuclear cells infiltration (M). On contrary, CHL coadministration with titanium returned heart to normal appearance at titanium 500 mg/kg (F) with slightly congested blood vessels at TiO₂ 1000 mg/kg (G) but inflammatory cells still exist at the highest dose as indicated by the presence of mononuclear cells (H), (H&E X 400).



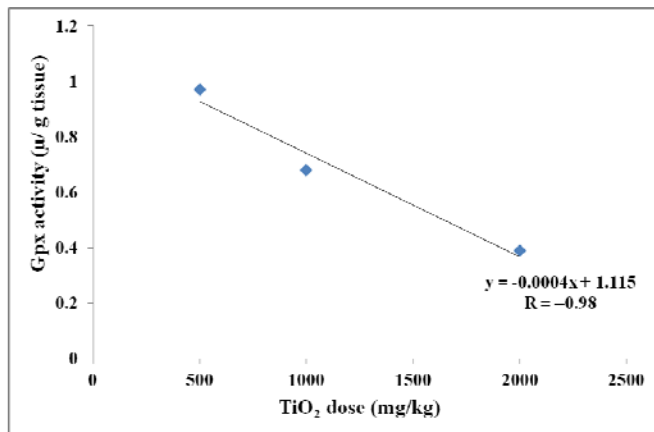


Figure 6: Regression lines and correlation coefficients for MDA and GSH levels and Gpx activity for mice injected i.p. by TiO₂ different doses. Results are expressed as mean

4. Discussion

TiO₂ nanoparticles are now in daily use in popular sunscreens, toothpastes, and cosmetics and in the environmental decontamination of air, soil, and water [34,35] that makes them widespread and its potential entry through various routes increasing their exposure risk to humans. Characterization of TiO₂ nanoparticles confirmed the purchased rutile and anatase form and their polyhedral morphology and evidenced that CHL did not affect on their physicochemical properties and still in the nanoscale range as nano-TiO₂ particles have nearly the same size either suspended in deionized dist. H₂O or in CHL solution (Fig. 1C) but CHL acted as a more suitable medium for nano-titanium dispersion as observed by the non-statistically smaller particle size in CHL compared with that in water. Therefore, the current study was designed to evaluate p53 mediated apoptosis and oxidative stress as a possible way for nano-TiO₂ induced cardiotoxicity and the possible protection by CHL co-administration in mice.

Despite inhalation and oral administration are the primary routes for nano-titanium exposure, it was injected i.p. in this study due to the recently wide use of TiO₂ nanoparticles in nanomedicine and pharmaceuticals as i.p. injection improves nanoparticles uptake compared to intravenous administration [7,36] Results of the current study confirmed the previously reported non genotoxic effects and safety use of CHL [19-21] by the observed non significant changes in heart DNA and architecture and was also further confirmed by the observed non-statically significant change in lipid peroxidation marker (MDA level) and antioxidant defense systems representing by GSH level and Gpx activity compared with the negative control value [37, 38].

Nano-TiO₂ cardiotoxicity was evidenced by the observed significant increases in DNA damage inductions indicating by significant increases in tail length, %tail DNA and tail moment at the tested doses in agreement with the previous studies [11, 14, 39]. Recently, oxidative stress was proposed as a possible indirect mechanism for nano-TiO₂ induced toxicity [40]. Our finding of the increased MDA level and the decreased GSH level and Gpx activity in nano-TiO₂ treated cardiac muscles confirmed the

previously reported oxidative stress and free oxygen radical generation by TiO₂ nanoparticles ([11,14,41]. Indeed, the decreases in Gpx activity confirmed the study of Chen *et al.* [7] showed that hydrogen peroxide (H₂O₂) is one of the predominant free radicals as Gpx detoxifies H₂O₂ to H₂O and O₂.

As generation of free oxygen radicals and oxidative stress triggers a host of cellular events, including DNA damage and apoptosis. Apoptosis, programmed cell death, is an important way to maintain the cellular homeostasis between cell division and cell death. Nano-TiO₂ induced apoptosis was evidenced in this study qualitatively by the formation of both ladder and smeared DNA on agarose gel in accordance with Alarifi *et al.* [40].

Moreover, the findings of the high incidence of mutations inductions in p53 exons (5-8) by the nano-TiO₂ different doses in this study speculated that nano-TiO₂ cardiotoxicity could be attributed to the p53 mediated apoptosis induction because p53 mutations in exons 5-8, independent of their type and location, resulting in loss of p53 function that associated with increased the incidence of apoptosis [42] in accordance with the previously reported Nano-TiO₂ induced apoptosis [11, 43, 44]. Additionally, the recorded oxidative stress and free oxygen radicals generation by TiO₂ nanoparticles resulting in up-regulation of p53 because the mutant p53 don't induce MDM-2 gene expression resulting in its accumulation at very high concentrations and also worse mutant p53 protein itself can inhibit normal p53 [45] thus genomic stability decreases with up-regulation of p53 gene leading to apoptosis in a harmony with [40, 46, 47]. The p53 exons (5-8) were chosen for SSCP analysis to screen for the presence of mutations because previous animal studies have shown that most p53 mutations occur in this region as it is more susceptible to strand breakage and hypomethylation and less highly conserved exonic regions of the p53 gene [48].

The observed strong correlation coefficients between the tested TiO₂ doses and its toxicity indicators including DNA damage inductions and oxidative stress biomarkers confirmed the previously reported [11,14] dose dependent manner of it and proposed that nano-titanium accumulation might be closely related to its cardiotoxicity.

The observed histopathological changes including edema, hemorrhage, hyalinosis, invasion of inflammatory cells including leucocytes and mononuclear cells and finally necrosis at the highest titanium dose further confirmed the nano-TiO₂ p53 mediated apoptosis in myocardial tissue in this study in a harmony with Sheng *et al.*, [14] who showed that titanium accumulation in heart led to sparse cardiac muscle fibers, inflammatory response, cell necrosis, and cardiac biochemical dysfunction. The observed infiltration of leucocytes and the presence of necrotic cells have been reported as indicators of oxidative stress [40, 49].

Oxidative stress could lead to further damage to cell membranes and proteins, including enzymes, which eventually results in loss of membrane fluidity and

function causing entrance of solutes and water leading to the observed edema. Moreover, the appearance of leucocytes and mononuclear cells in myocardium confirmed the previously reported oxidative stress role in increased apoptotic rate by participating in both the initiation and signalling of the apoptotic process of mononuclear cells [50] by the observed significant reductions in GSH level that acts as cytosolic thiol and sustains the apoptotic signalling together with other events such as changes in the control of cytosolic Ca² homeostasis and Gpx activity inhibition and further oxidant stress. However, this controlled disruption of cytosolic thiol eg. GSH homeostasis can be reversed with a full 'rescue' of cell function and viability. Accordingly, thiol suppliers such as N-acetylcysteine or other antioxidants such as vitamin E could be used to down-regulate apoptosis in different cell models [51,52]. Therefore, CHL was used in this study as a trial to decreased TiO₂ induced apoptosis.

CHL co-administration with nano-TiO₂ nanoparticles resulting in significant reductions in TiO₂ induced cardiotoxicity as manifested by the recorded significant decreases in ROS generation and induction of p53 mediated apoptosis. Despite CHL have several mechanisms for its protective effects against mutagens and clastogens including scavenging free radicals, binding to the active site of mutagen, and adsorbing or absorbing toxic compounds [20,53]. Our results confirmed the reported antioxidative property of CHL [37,54] by the observed MDA depletion and restoring antioxidant defense system GSH level and GPx activity in concurrent with the recorded significant decreased DNA damage inductions. Similar results were observed by **Boloor et al.** [55] who showed that CHL inhibits lipid peroxidation by scavenging free radicals and restores depleted levels of SOD and GSH suggesting the role of CHL in quenching the ROS formed.

Moreover, **Kumar et al.** [56] assumed that the protection by CHL should be arising mainly due to the scavenging of hydroxyl radicals by its copper and magnesium that inhibit lipid peroxidation due to scavenging (repairing) the tyrosyl radical or inhibiting myeloperoxidase (MPO) by reduced dityrosine formation [57].

The previously reported CHL antimutagenic effect against p53 gene mutations by **Gradecka-Meesters et al.**, [58] was further evidenced in this study by the observed decrease in the incidence of p53 mutation induction. Attenuation of nano-TiO₂ induced p53 mediated apoptosis by CHL co-administration as evidenced by the ladder DNA disappearance and appearance of p53 mutations only at the highest titanium dose could be attributed to the previous reported CHL ROS scavenging ability that enhances antioxidant defense system [37,57] because the elevated GSH level acts as co-substrate providing thiol group for the possible Gpx detoxifications reactions [59,60]. GPx detoxifies H₂O₂ to H₂O and O₂, and converts lipid hydroperoxides to nontoxic alcohols that guard against oxidative damage induced by ROS [61].

In conclusion: the observed nano-titanium induced cardiotoxicity could be attributed to the oxidative stress and p53 mediated apoptosis in a dose dependent manner that ameliorated by CHL co-administration via its free radical scavenger ability.

Acknowledgment

I would like to express my most sincere gratitude my faculty of Science and Cairo University for providing me chemicals and instruments.

References

- [1] Mallik A, Bryan S, Puukila S, Chen A and Khaper N. Efficacy of Pt-modified tio₂ nanoparticles in cardiac cells. *Exp Clin Cardiol*; 2011; **16** (1):6-10.
- [2] Xu J, Shi H, Ruth M, Yu H, Lazar L, Zou B, Yang C, Wu A and Zhao J. Acute Toxicity of Intravenously Administered Titanium Dioxide Nanoparticles in Mice. *PLoS*; 2013; **8**(8): 70618-70626
- [3] Warheit D.B, Hoke R. A., Finlay C, Donner E. M, Reed K L., Sayes C M.. Development of a base set of toxicity tests using ultrafine TiO₂ particles as a component of nanoparticle risk management. *Toxicol Lett*; 2007: **171**: 99–110
- [4] Wang J., Zhou G., Chen C., Yu H., Wang T., Ma Y., Jia G., Gao Y., Li B., Sun J., Li Y., Jiao F., Zhao Y. and Chai Z. Acute toxicity and biodistribution of different sized titanium dioxide particles in mice after oral administration. *Toxicol Lett* ; 2007: **168** (2): 176-85.
- [5] Bermudez, E., Mangum, J. B., Wong, B. A., Asgharian, B., Hext, P. M., Warheit, D. B., Everitt, J. I., and Moss, O. R.. Pulmonary responses of mice, rats, and hamsters to subchronic inhalation of ultrafine titanium dioxide particles. *Toxicol. Sci.*; 2004: **77**: 347–357.
- [6] Thomas T, Thomas K, Sadrieh N, Savage N, Adair P and Bronaugh R. Research strategies for safety evaluation of nanomaterials, part VII: evaluating consumer exposure to nanoscale materials. *Toxicol Sci.*;2006: **91**: 14–19
- [7] Chen J, Dong X, Zhao J and Tang G. *In vivo* acute toxicity of titanium dioxide nanoparticles to mice after intraperitoneal injection. *J. Appl. Toxicol.*; 2009: **29**(4):330-337
- [8] Song W, Wang J, Liu M, Li P, Zhou G, Li Z and FanY. Research Article: Titanium Dioxide Nanoparticles Induced Proinflammation of Primary Cultured Cardiac Myocytes of Rat. *J. of Nanomat*; 2013: **13**:1-9 pages.
- [9] Liu H, Ma L, Zhao J, Liu J, Yan J, Ruan J and Hong F. Biochemical toxicity of nano-anatase TiO₂ particles in mice. *Biol Trace Elem Res.*; 2009: **129** (1-3):170-80
- [10] Wang J, Fan Y, Gao Y, Hu Q and Wang T. TiO₂ nanoparticles translocation and potential toxicological effect in rats after intraarticular injection. *Biomaterials*; 2009: **30**:4590–600.
- [11] Faddah LM, Abdel Baky NA, Al-Rasheed NM and Al-Rasheed NM. Full Length Research Paper: Biochemical responses of nanosize titanium dioxide in

- the heart of rats following administration of idepenone and quercetin. *African J. of Pharm and Pharmacol*; 2013; **7(38)**: 2639-2651
- [12] Peters A, Dockery DW, Muller JE and Mittleman MA. Increased particulate air pollution and the triggering of myocardial infarction. *Circulation*; 2001: **103**:2810-2815. Ajith, T.A.; Usha, S. and Nivitha, V. (2007). Ascorbic acid and α -tocopherol protect anticancer drug cisplatin induced nephrotoxicity in mice: a comparative study. *Clinica. Chimica. Acta.*, **375**: 82 – 86
- [13] Guo LL, Liu XH, Qin DX, Gao L, Zhang HM, Liu JY and Cui YG. Effects of nanosized titanium dioxide on the reproductive system of male mice. *Zhonghua Nan Ke Xue.*; 2009: **15 (6)**:517-22.
- [14] Sheng L, Wang X, Sang X, Ze Y, Zhao X, Liu D, Gui S, Sun Q, Cheng J, Cheng Z, Hu R, Wang L and Hong F. Cardiac oxidative damage in mice following exposure to nanoparticulate titanium dioxide. *J. of Biomed Mat Res Part A*; 2013: **101(11)**: 3238–3246
- [15] Premkumar, K.; Abraham, S.K.; Santhiya, S.T. and Ramesh, A. Protective effect of *siprulina fusiformis* on chemical-induced genotoxicity in mice. *Fitoterapia*; 2004: **75**: 24 – 31
- [16] Baillie J.K., Thompson A.A.R., Irving J.B., Bates M.G.D., Sutherland A.I., MacNee W., Maxwell S.R.J. and Webb D.J. "Oral antioxidant supplementation does not prevent acute mountain sickness: double blind, randomized placebo-controlled trial". *QJM102*; 2009: **(5)**: 341–8. Alarifi S, Ali D, Al-Doaiss AA, Ali BA, Ahmed M, Al-Khedhairi AA (2013). Histologic and apoptotic changes induced by titanium dioxide nanoparticles in the livers of rats. *International Journal of Nanomedicine*; 8: 3937–3943
- [17] Sarkar, D.; Sharma, A. and Talukder, G. Chlorophyll and chlorophyllin as modifiers of genotoxic effects. *Mut Res.*; 1994: **318**: 239 – 247. Bez, G.C.; Jordao, B.Q.; Vicentini, V.E.P. and Mantovani, M.S. (2001). Investigation of genotoxic and antigenotoxic activities of chlorophylls and chlorophyllin in cultured V79 cells. *Mut Res.*, **497**: 139 – 145
- [18] Bez, G.C.; Jordao, B.Q.; Vicentini, V.E.P. and Mantovani, M.S. Investigation of genotoxic and antigenotoxic activities of chlorophylls and chlorophyllin in cultured V79 cells. *Mut Res.*; 2001: **497**: 139 – 145
- [19] Negraes, P.D.; Jorao, B.Q.; Vicentini, V.E.P. and Mantovani, M.S. Anticlastogenicity of chlorophyllin in the different cell cycle phases in cultured mammalian cells. *Mut Res.*; 2004: **557**: 177 – 182
- [20] Hayatsu H, Negishi T, Arimoto-Kobayashi S. Chemoprevention of cancer and DNA damage by dietary factors. *Weinheim: Wiley-VCH*; 2009: Pp 699–708.
- [21] Leite VS, Oliveira RJ, Kanno TY, Mantovani MS, Moreira EG and Salles MJ. Chlorophyllin in the intra-uterine development of mice exposed or not to cyclophosphamide. *Acta Scientiarum. Health Sciences. Maringá*; 2013: **35(2)**: 201-210
- [22] Garcia-Rodriguez M.C, Lopez-Santiago V. and Altamirano-Lozano M. Effect of chlorophyllin on chromium trioxide-induced micronuclei in polychromatic erythrocytes in mouse peripheral blood. *Mut Res*; 2001: **496**: 145 – 151
- [23] De Vogel J, Jonker-Termont D.S.M.L, Katan M.B. and der Meer R.V. Nutrition and Cancer: Natural chlorophyll but not chlorophyllin prevents heme-induced cytotoxic and hyperproliferative effects in rat colon. *American Society for Nutritional Sciences. J. Nutr.*; 2005: **135**: 1995 – 2000
- [24] Ibrahim M A, Elbehairy A M, Ghoneim MA and Amer H A.. Protective effect of curcumin and chlorophyllin against DNA mutation induced by cyclophosphamide or benzo[a]pyrene. *Z Naturforsch C*; 2007: **62 (1)**: 215-222
- [25] Tice R.R., Agurell E., Anderson V, Burlinson B., Hartmann A., Kobayashi H., Miyamae Y., Rojas E., Ryu J.C. and Sasaki Y.F. Single cell gel/comet assay: guidelines for in vitro and in vivo genetic toxicology testing. *Environ. Mol. Mutagen*; 2000: **35**: 206–221.
- [26] Sriram MI, Kanth SBM, Kalishwaralal K and Gurunathan S. Antitumor activity of silver nanoparticles in Dalton's lymphoma ascites tumor model. *Int. J of Nanomed*; 2012: **5**: 753–762
- [27] Biase F.H., Franco M.M., Goulart L.R. and Antunes R.C. Protocol for extraction of genomic DNA from swine solid tissue. *Genetics and Molecular Biology*; 2002: **25(3)**: 313-315
- [28] Gutierrez M.I, Bhatia K, Siwarski D, Wolff L, Magrath I.T, Mushinski J.F and Huppil K.. Infrequent p53 Mutation in Mouse Tumors with Deregulated myc. *Cancer Res*; 1992: **52**: 1032-1035.
- [29] Gasser R.B, Hu M, Chilton N.B, Campbell B.E, Jex A.J, Otranto D, Cafarchia C, Beveridge I & Zhu X. Single-strand conformation polymorphism (SSCP) for the analysis of genetic variation. *Nature protocol*; 2006: **(6)**: 3121-3128
- [30] Ohkawa H, Ohishi W and Yagi K. Assay for lipid peroxides in animal tissues by thiobarbituric acid reaction. *Anal. Biochem*; 1979: **95**: 351-8
- [31] Ellman, G.L. Tissue sulfhydryl groups. *Arch. Biochem. Biophys.*; 1959: **17**: 214 – 226
- [32] Paglia D.e and Valentine W.N. Studies on the quantitative and qualitative characterization of erythrocyte glutathione peroxidase. *J. Lab Clin Med* ; 1967: **70**: 158-169
- [33] Statistical Analyses Systems (SAS). SAS Program ver. 9.12, SAS institute incorporation, Cary, NC 27513 USA; 2005
- [34] Choi H, Stathatos E and Dionysiou DD. Sol-gel preparation of mesoporous photocatalytic TiO₂ films and TiO₂/Al₂O₃ composite membranes for environmental applications. *Appl. Catal. B-Environ.*; 2006: **63**:60–67
- [35] Hu C.W., Lia M, Cui Y.B., Li D.S., Chen J and Yang L.Y. Toxicological effects of TiO₂ and ZnO nanoparticles in soil on earthworm *Eisenia fetida*. *Soil Biology & Biochemistry*; 2010: **42**: 586-591
- [36] Jung C, Kaul MG, Bruns OT, Dučić T, Freund B, Heine M, Reimer R, Meents A, Salmen SC, Weller H, Nielsen P, Adam G, Heeren J and Ittrich H. Intraperitoneal Injection Improves the Uptake of Nanoparticle Labeled HDL to Atherosclerotic Plaques Compared to Intravenous Injection: A Multimodal

- Imaging Study in ApoE^{-/-} Mice. *Circ. Card. Vascul. Imaging*; 2013: 1942-80
- [37] Kumar SS, Shankar B and Sainis KB. Effect of chlorophyllin against oxidative stress in splenic lymphocytes in vitro and in vivo. *Biochim Biophys Acta*; 2004: **1672**: 100–111.
- [38] Osowski A, Pietrzak M, Wieczorek Z and Wieczorek J. "Natural compounds in the human diet and their ability to bind mutagens prevents DNA-mutagen intercalation". *J. of Toxicol. and Environmental Health, Part A*; 2010: **73 (17-18)**: 1141–1149.
- [39] Moon C, Park HJ, Choi YH, Park EM, Castranova V and Kang JL. Pulmonary inflammation after intraperitoneal administration of ultrafine titanium dioxide (TiO₂) at rest or in lungs primed with lipopolysaccharide. *J Toxicol Environ Health A*; 2010: **73 (5)**: 396-409
- [40] Alarifi S, Ali D, Al-Doaiss AA, Ali BA, Ahmed M, Al-Khedhairi AA. Histologic and apoptotic changes induced by titanium dioxide nanoparticles in the livers of rats. *Int J of Nanomedicine*; 2013: **8**: 3937–3943
- [41] Kang SJ, Kim BM, Lee YJ, Chung HW. Titanium dioxide nanoparticles trigger p53-mediated damage response in peripheral blood lymphocytes. *Environ. Mol.*; 2008: **49(5)**:399-405.
- [42] Slooten H-J V, van de Vijver MJ, Børresen N-L, Eyfjörd JE, Valgardsdóttir R, Scherneck S, Nesland JM, Devilee P, Cornelisse CJ, van Dierendonck JH. Mutations in exons 5–8 of the *p53* gene, independent of their type and location, are associated with increased apoptosis and mitosis in invasive breast carcinoma. *The J of Pathol*; 1999: **189(4)**: 504–513
- [43] Ma L, Zhao J, Wang J, Liu J, Duan Y, Liu H, Li N, Yan J, Ruan J, Wang H, Hong F. The Acute Liver Injury in Mice Caused by Nano-Anatase TiO₂. *Nanoscale Res Lett*; 2009: **4**:1275–1285
- [44] Li N, Ma LL, Wang J, Liu J, Duan YM, Liu HT, Zhao XY, Wang SS, Wang H, Hong FS. Interaction between nano-anatase TiO₂ and liver DNA from mice *in vivo*. *Nanoscale Res. Lett.*; 2010: **5**:108–115.
- [45] Blagosklonny, MV.. P53: An ubiquitous target of anticancer drugs. *Intl J of Can*; 2002: **98**:161-166
- [46] French J.E., Lacks G.D., Trempus C., Dunnik J.K., Foley J., Mahler J., Tice R.R. and Tennant R.W.. Loss of heterozygosity frequency at the Trp53 locus in p53-deficient (+/-) mouse tumors is carcinogen- and tissue-dependent. *Carcinogenesis*; 2001: **21(1)**: 99-106
- [47] Modur V, Nagarajan R, Evers BM, Milbrandt J. FOXO proteins regulate tumor necrosis factor-related apoptosis inducing ligand expression. Implications for PTEN mutation in prostate cancer. *J Biol Chem*; 2002: **277**:47928–47937.
- [48] Liu Z, Choi S-W, Crott J.W., Smith D.E and Mason J.B. Multiple B-vitamin inadequacy amplifies alterations induced by folate depletion in *p53* expression and its downstream effector *MDM2*. *Int J Can*; 2008: **123(3)**: 519–525.
- [49] Hassan, H.M. and Fridovich, I. Chemistry and biochemistry of superoxide dismutases. *Eur. J. Rheumatol. Inflamm*; 1991: **4**: 160 – 172
- [50] Galli F, Ghibelli L, Buoncrisiani U, Bordoni V, D'Intini V, Benedetti S, Canestrari F, Ronco C and Floridi A. Mononuclear leukocyte apoptosis in haemodialysis patients: the role of cell thiols and vitamin E. *Nephrol Dial Transplant*; 2003:**18**: 1592–1600
- [51] Ricciarelli R, Tasinato A, Clement S, Ozer NK, Boscoboinik D and Azzi A. Tocopherol specifically inactivates cellular protein kinase C_β by changing its phosphorylation state. *Biochem J*; 1998: **15**: 243–249
- [52] Galli F, Rovidati S, Benedetti S et al. Lipid peroxidation, leukocyte function and apoptosis in hemodialysis patients treated with vitamin E-modified filters. *Contrib Nephrol*; 1999: **127**: 156–171
- [53] Sarkar, D.; Sharma, G. and Talukder, G. Chlorophyll and chromosome breakage. *Mut Res.*; 1996: **360**: 187 – 191
- [54] Zhang, Y; Guan, L; Wang, X; Wen, T; Xing, J and Zhao, J. Protection of chlorophyllin against oxidative damage by inducing HO-1 and NQO1 expression mediated by PI3K/Akt and Nrf2. *Free Radic Res.*; 2008: **42**:362-371
- [55] Bolloor, K.K.; Kamat, J.P and Devasagayam, T.P. Chlorophyllin as a protector of mitochondrial membrane against γ -radiation and photosensitization. *Toxicology*; 2000: **155**: 63 – 71
- [56] Kumar, S.S.; Chaubey, R.C.; Priyadarsini, K.I.; Devasagayam, T.P.A. and Chauhan, P.S. Inhibition of radiation-induced DNA damage in plasmid pBR322 by chlorophyllin and possible mechanis(s) of action. *Mut Res.*; 1999: **425**: 71 – 79
- [57] Kapiotis, S.; Hermann, M.; Exner, M.; Laggner, H. and Gmeiner, B.M.K. Copper-and magnesium protoporphyrin complexes inhibit modification of LDL induced by hemin, transition metal ions and tyrosyl radicals. *Free Radica. Res.*; 2005: **39**: 1193 – 1202
- [58] Gradecka-Meesters D, Palus J, Prochazka G, Segerbäck D, Dziubałtowska E, Kotova N, Jenssen D, Arkusz J, Lundin C, Vikström E, Rydzynski K, Nilsson R and Stępnik M. Assessment of the protective effects of selected dietary anticarcinogens against DNA damage and cytogenetic effects induced by benzo[a]pyrene in C57BL/6J mice. *Food Chem Toxicol.* ; 2011: 49(8):1674-83.
- [59] Mansour M.A., Mohmoud N.N., El-Khatib A.S. and Al-Bekairi A.M. Effects of thymoquinone on antioxidant enzyme activities, lipid peroxidation and DT-diaphorase in different tissues of mice: a possible mechanism of action. *Cell Biochem. Funct* ; 2002: **20**: 143-151
- [60] Ajith, T.A.; Usha, S. and Nivitha, V. Ascorbic acid and α -tocopherol protect anticancer drug cisplatin induced nephrotoxicity in mice: a comparative study. *Clinica. Chimica. Acta.*; 2007: **375**: 82 – 86
- [61] Watson AM, Warren G, Howard G, Shedlofsky SI and Blouin RA. Activities of conjugating and antioxidant enzymes following endotoxin exposure, *J Biochem Mol Toxicol*; 1999: **13**, 63-9